

Research Article

Effect of pH on the Characteristics of $\text{Cu}_2\text{ZnSnS}_4$ Nanoparticles

R. Lydia and P. Sreedhara Reddy

Department of Physics, Sri Venkateswara University, Tirupati 517502, India

Correspondence should be addressed to P. Sreedhara Reddy; psreddy4@gmail.com

Received 17 April 2013; Accepted 14 May 2013

Academic Editors: H. D. Hochheimer, C. Homes, A. N. Kocharian, A. McGurn, and A. Oyamada

Copyright © 2013 R. Lydia and P. Sreedhara Reddy. This is an open access article distributed under the Creative Commons Attribution License, which permits unrestricted use, distribution, and reproduction in any medium, provided the original work is properly cited.

We have investigated the effect of pH on the structural and optical properties of chemical coprecipitated $\text{Cu}_2\text{ZnSnS}_4$ (CZTS) nanoparticles. The CZTS nanoparticles have been successfully synthesized at different pH values ranging from 6 to 9, keeping all other deposition parameters as constant. X-ray diffraction and Raman studies confirmed the Kesterite structure. The powders synthesized at a pH value of 8 exhibited preferred orientation along (112) and (220) with near stoichiometric ratio. The as synthesized nanoparticles exhibited direct band gap of 1.4 eV which is an optimum value for the absorber layer in the fabrication of photovoltaic cells.

1. Introduction

In the last five decades, the properties of bulk materials have been investigated and understood in great detail. But now a great deal of research interest has been turned on the preparation and characterization of nanoparticles for their unique size-dependent electrical and optical properties. Nanotechnology has recently attracted more interest in the fields of photovoltaics, electrooptical devices and sensors, and so forth. Traditionally, CuInGaSe_2 (CIGS) and CuInSe_2 (CIS) have been used as absorber layer in solar cells because of their high conversion efficiency (20%) [1]. But the utilization of these materials in large scale solar cell production could cause an environmental problem due to the toxic nature of selenium and expensive raw materials. To overcome these difficulties, alternative search for absorber layers is still ongoing. Recently the copper zinc tin sulphide (CZTS) nanoparticles have attracted researchers with their unique properties, and they play crucial role in the application of absorber layer in the solar cell. The elements of CZTS are earth abundant, inexpensive, environmental friendly, nontoxic, and pollution-free [2]. CZTS has optimum band gap of 1.4 eV to 1.5 eV which is suitable for photovoltaic applications [3]. CZTS has high absorption coefficient $>10^4 \text{ cm}^{-1}$ [4]. Theoretical conversion efficiency of CZTS solar cell is 32.2% [5]. The CZTS solar cell exhibits a conversion efficiency of 10% [6]. Only limited work

was carried out on the preparation and characterization of bulk CZTS [7–11]. But due to the advantages of nanoparticles, in this present work we are synthesizing CZTS nanoparticles.

Among many physical methods [12–15] and chemical methods [16–25], chemical coprecipitation method has great advantages in preparing CZTS nanoparticles due to inexpensive apparatus, low power consumption, nontoxic byproducts, high homogeneous, high flexibility, effective size control, and absence of the need of vacuum technique, and this makes such technique more suitable and economical for large scale production. In the present work, we have focused our attention on the effect of pH on the structural and optical properties of the CZTS nanoparticles.

2. Experimental

To prepare CZTS nanoparticles the chemicals, $(\text{C}_5\text{H}_8\text{O}_2)_2\cdot\text{Cu}$, $(\text{C}_5\text{H}_8\text{O}_2)_2\text{SnBr}_2$, $(\text{CH}_3\text{COO})_2\text{Zn}\cdot 2\text{H}_2\text{O}$, and $\text{H}_2\text{N}\cdot\text{CS}\cdot\text{NH}_2$ were purchased from Sigma Aldrich in the purest form available and with no need for further purification. The CZTS nanoparticles were synthesized by chemical coprecipitation method with an aqueous solution containing 1.5 mmol of $(\text{C}_5\text{H}_8\text{O}_2)_2\cdot\text{Cu}$, 0.75 mmol of $(\text{C}_5\text{H}_8\text{O}_2)_2\text{SnBr}_2$, 0.75 mmol of $(\text{CH}_3\text{COO})_2\text{Zn}\cdot 2\text{H}_2\text{O}$, and 3 mmol of $\text{H}_2\text{N}\cdot\text{CS}\cdot\text{NH}_2$. Oleylamine is taken as a solvent. In order to change the pH

value of the solution, a few drops of diluted ammonia solution were added to the aqueous solution. The experiment was carried out with solutions having pH values 6, 7, 8, and 9. The solutions were stirred for 4 hours at constant synthesis temperature 150°C. After stirring the solutions, the precipitate was collected and washed with ethanol for 4 to 5 times to remove byproducts. The precipitates were annealed at constant temperature 100°C. Finally, by grinding the precipitates, we get black colored CZTS nanopowder.

The structure and crystallinity of the CZTS nanoparticles were analysed using X-ray diffraction technique. This analysis was done with a Seifert 3003 TT X-ray diffractometer with Cu K α radiation ($\lambda = 0.1546$ nm). Raman spectroscopic studies of these nanoparticles were carried out using LabRam HR800 Raman spectrometer. Scanning electron micrographs were obtained using scanning electron microscopy (SEM) of model EVO MA 15 manufactured by Carl Zeiss. The compositional studies of these nanoparticles were obtained from energy dispersive spectroscopy (EDS) attached with SEM of model Oxford instruments Inca Penta FETx3. In order to study optical properties of these nanoparticles, the absorption measurements were carried out by using a Perkin Elmer Lambda 950 UV-VIS-NIR spectrophotometer with a wavelength resolution better than 0.2 nm at room temperature.

3. Results and Discussion

3.1. Structural Characterization. XRD measurements were performed for all the nanopowders to observe the structure of CZTS nanoparticles. The diffraction data was collected at 2θ values ranging from 20-to 70-degree diffraction angles. Figure 1 shows the X-ray diffraction patterns of the CZTS nanoparticles at different pH values. The diffraction profiles indicated that the samples synthesized with pH 6 and 7 have peaks at 28.59°, which corresponds to the orientations along (112) with low intensity, and the sample with pH 8 have peaks at 28.59°, 47.44°, corresponds to (112), (220) planes with high intensity of Kesterite structure of CZTS (JCPDS 26-0575), which was in good agreement with the previous reports [26–28]. The sample with pH 9 exhibited (311)* plane which corresponds to the Cu_xS phase according to the JCPDS data (JCPDS 89-2073). The lattice parameters of the CZTS nanoparticles with pH values 6, 7, and 8 were found to be $a = 0.5427$ nm and $c = 1.0848$ nm which are in agreement with the reported data. From these X-ray diffraction studies, we concluded that CZTS phase with better crystallinity was observed when the powders were synthesized at a pH of 8.

XRD studies will be completed only after taking the Raman characterization in to account. Raman measurements could be used to confirm the structure of the CZTS nanoparticles. Figure 2 displays the Raman spectra of the CZTS nanoparticles.

From Figure 2, the Raman peak was observed at 334 cm⁻¹ for the samples with pH values 6, 7, and 8, which corresponds to the tetragonal structure of the CZTS. This peak was in good agreement with the CZTS [29, 30]. The sample with the pH 9 shows the Raman peak at 418 cm⁻¹ corresponds to Cu_xS. This

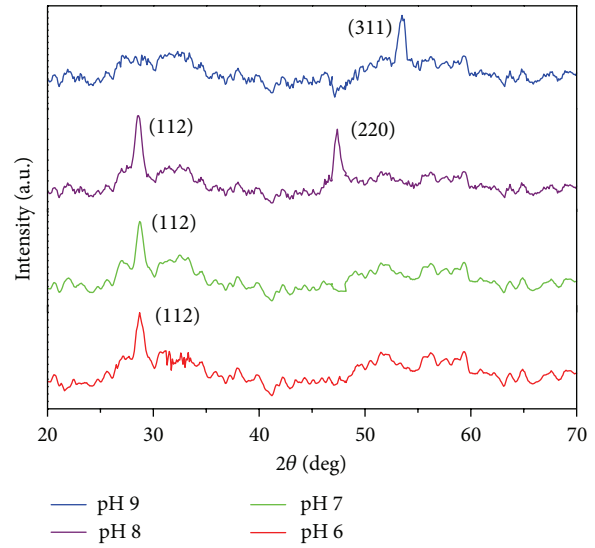


FIGURE 1: X-ray diffraction patterns of the CZTS nanoparticles with different pH values.

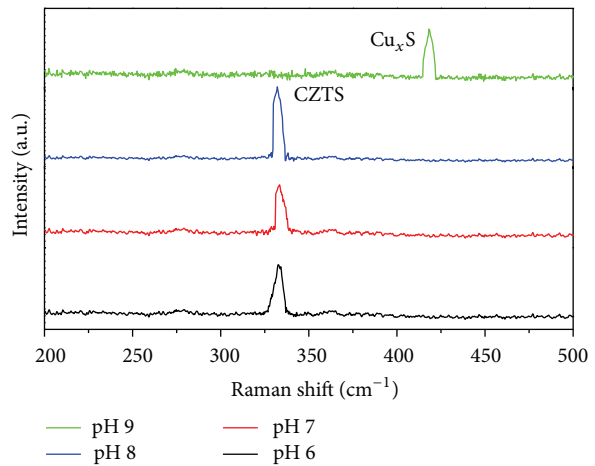


FIGURE 2: Raman scattering spectra of CZTS nanoparticles.

Raman data was in good agreement with the previous XRD studies. The CZTS structure was not found with the pH value 9. Therefore, it can be concluded that the pH of the sample strongly affects the formation of the CZTS nanoparticles.

Scanning electron microscopy (SEM) was used to study the surface morphology of CZTS nanoparticles. Figure 3 displays the SEM images of the CZTS nanoparticles with different pH values. It was observed that the morphology of the nanoparticles with pH values of 6 and 7 has slightly distinct grains with round shape, sample with pH 8 has distinct grains with round shape, and surface morphology was smeary for the sample with pH 9.

3.2. Composition Analysis. The EDS technique was used to estimate the elemental composition of the CZTS nanoparticles. Figure 4 shows the typical image of the elemental

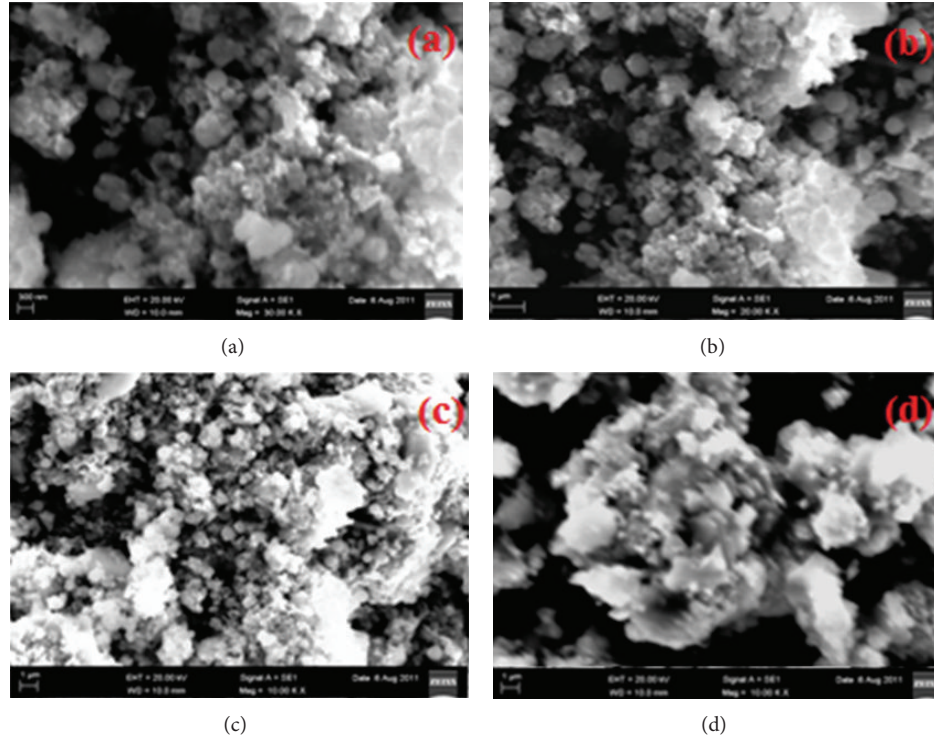


FIGURE 3: SEM images of CZTS nanoparticles: (a) pH = 6, (b) pH = 7, (c) pH = 8, and (d) pH = 9.

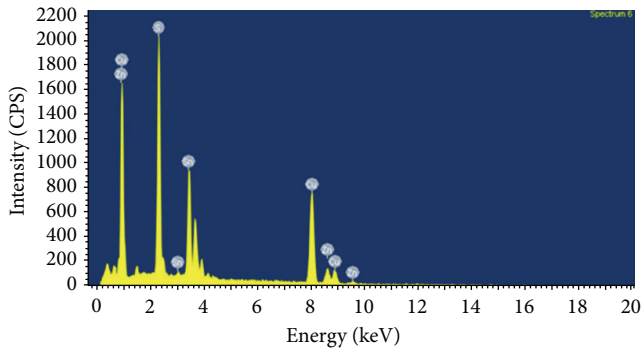


FIGURE 4: EDS spectra of CZTS nanoparticles with pH 8.

composition of the CZTS nanoparticles. From this compositional study, it was noticed that the concentration of the copper was increased with the increase of pH [24]. The increase in the concentration of the copper was less with the increase of pH from 6 to 8. The concentration change in the copper was more while going from pH 8 to pH 9. The CZTS nanoparticles with pH 8 reached near stoichiometry.

3.3. Optical Properties. Optical band gap of CZTS nanoparticles was drawn from $(\alpha h\nu)^2$ Vs photon energy by extrapolating the straight line portion of the graph in the higher absorption region, where α and $h\nu$ are absorption coefficient and photon energy, respectively. Figure 5 shows the band gap plots of CZTS nanoparticles with different pH values.

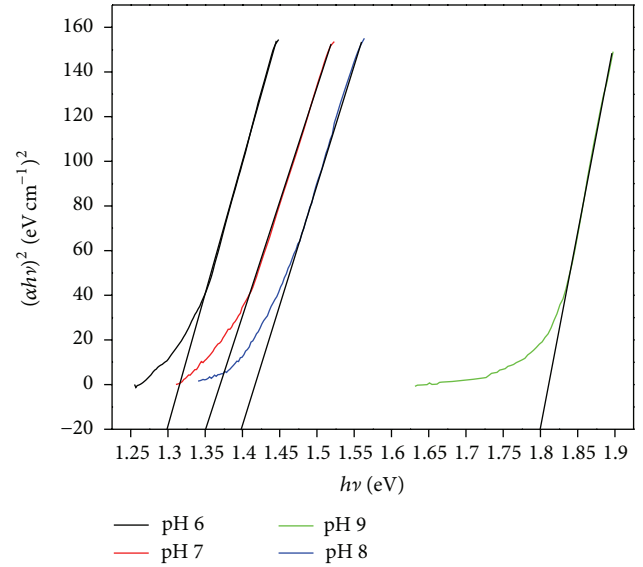


FIGURE 5: The band gap images of the sample with pH values 6, 7, 8, and 9.

From the graph it was observed that the band gap of the CZTS nanoparticles varied from 1.3 to 1.8 eV. Direct band gap values of samples with pH values 6, 7, and 8 were found to be 1.3 eV, 1.35 eV, and 1.4 eV, respectively [3]. However, the sample with pH 9 has band gap 1.8 eV which corresponds to the Cu_2S [31]. The change in the optical band gap of this sample is due to compositional difference.

4. Conclusions

CZTS nanoparticles were successfully synthesized by chemical coprecipitation method by varying pH value of the solution from 6 to 9. CZTS nanoparticles with pH values 6, 7, and 8 exhibited Kesterite structure with preferential orientations. The sample with pH 8 reached near stoichiometry. The optimum band gap of the CZTS is 1.4 eV. From the previous results and discussions, it seems that the pH will strongly affect the structural and optical properties of the CZTS nanoparticles. The CZTS nanoparticles with pH 8 will be perfectly suitable for the application of the absorber layer of the solar cell.

Acknowledgment

The authors would like to express their thanks to the University Grants Commission (UGC), New Delhi, for awarding UGC-BSR Fellowship in Sciences for Meritorious Students.

References

- [1] H. Katagiri, K. Jimbo, W. S. Maw et al., "Development of CZTS-based thin film solar cells," *Thin Solid Films*, vol. 517, no. 7, pp. 2455–2460, 2009.
- [2] H. Katagiri, K. Jimbo, S. Yamada et al., "Enhanced conversion efficiencies of $\text{Cu}_2\text{ZnSnS}_4$ -based thin film solar cells by using preferential etching technique," *Applied Physics Express*, vol. 1, no. 4, pp. 0412011–0412012, 2008.
- [3] K. Ito and T. Nakazawa, "Electrical and optical properties of stannite-type quaternary semiconductor thin films," *Japanese Journal of Applied Physics*, vol. 27, no. 11, pp. 2094–2097, 1988.
- [4] H. Katagiri, "Cu₂ZnSnS₄ thin film solar cells," *Thin Solid Films*, vol. 480–481, pp. 426–432, 2005.
- [5] H. Yoo and J. Kim, "Comparative study of $\text{Cu}_2\text{ZnSnS}_4$ film growth," *Solar Energy Materials and Solar Cells*, vol. 95, no. 1, pp. 239–244, 2011.
- [6] T. K. Todorov, K. B. Reuter, and D. B. Mitzi, "High-efficiency solar cell with earth-abundant liquid-processed absorber," *Advanced Materials*, vol. 22, no. 20, pp. E156–E159, 2010.
- [7] G. P. Bernardini, D. Borriani, A. Caneschi et al., "EPR and SQUID magnetometry study of $\text{Cu}_2\text{FeSnS}_4$ (stannite) and $\text{Cu}_2\text{ZnSnS}_4$ (kesterite)," *Physics and Chemistry of Minerals*, vol. 27, no. 7, pp. 453–461, 2000.
- [8] P. Bonazzi, L. Bindi, G. P. Bernardini, and S. Menchetti, "A model for the mechanism of incorporation of Cu, Fe and Zn in the stannite—Kesterite series, $\text{Cu}_2\text{FeSnS}_4$ – $\text{Cu}_2\text{ZnSnS}_4$," *Canadian Mineralogist*, vol. 41, no. 3, pp. 639–647, 2003.
- [9] F. Di Benedetto, G. P. Bernardini, D. Borriani, W. Lottermoser, G. Tippelt, and G. Amthauer, "57Fe- and 119Sn- Mössbauer study on stannite ($\text{Cu}_2\text{FeSnS}_4$)-kesterite ($\text{Cu}_2\text{ZnSnS}_4$) solid solution," *Physics and Chemistry of Minerals*, vol. 31, no. 10, pp. 683–690, 2005.
- [10] K. Tanaka, Y. Miyamoto, H. Uchiki, K. Nakazawa, and H. Araki, "Donor-acceptor pair recombination luminescence from $\text{Cu}_2\text{ZnSnS}_4$ bulk single crystals," *Physica Status Solidi A*, vol. 203, no. 11, pp. 2891–2896, 2006.
- [11] S. Schorr, H. Hoebler, and M. Tovar, "A neutron diffraction study of the stannite-kesterite solid solution series," *European Journal of Mineralogy*, vol. 19, no. 1, pp. 65–73, 2007.
- [12] K. Tanaka, D. Kawasaki, M. Nishio, Q. Guo, and H. Ogawa, "Donor-acceptor pair recombination luminescence from $\text{Cu}_2\text{ZnSnS}_4$ bulk single crystals," *Physica Status Solidi A*, vol. 3, pp. 2844–2896, 2006.
- [13] A. Weber, H. Krauth, S. Perl et al., "Multi-stage evaporation of $\text{Cu}_2\text{ZnSnS}_4$ thin films," *Thin Solid Films*, vol. 517, no. 7, pp. 2524–2526, 2009.
- [14] K. Sekiguchi, K. Tanaka, K. Moriya, and H. Uchiki, "Epitaxial growth of $\text{Cu}_2\text{ZnSnS}_4$ thin films by pulsed laser deposition," *Physica Status Solidi C*, vol. 3, no. 8, pp. 2618–2621, 2006.
- [15] K. Moriya, K. Tanaka, and H. Uchiki, "Cu₂ZnSnS₄ thin films annealed in H₂S atmosphere for solar cell absorber prepared by pulsed laser deposition," *Japanese Journal of Applied Physics*, vol. 47, no. 1, pp. 602–604, 2008.
- [16] K. Moriya, J. Watabe, K. Tanaka, and H. Uchiki, "Characterization of $\text{Cu}_2\text{ZnSnS}_4$ thin films prepared by photo-chemical deposition," *Physica Status Solidi C*, vol. 3, no. 8, pp. 2848–2852, 2006.
- [17] K. Tanaka, N. Moritake, and H. Uchiki, "Preparation of $\text{Cu}_2\text{ZnSnS}_4$ thin films by sulfurizing sol-gel deposited precursors," *Solar Energy Materials and Solar Cells*, vol. 91, no. 13, pp. 1199–1201, 2007.
- [18] Y. Miyamoto, K. Tanaka, M. Oonuki, N. Moritake, and H. Uchiki, "Optical properties of $\text{Cu}_2\text{ZnSnS}_4$ thin films prepared by sol-gel and sulfurization method," *Japanese Journal of Applied Physics*, vol. 47, no. 1, pp. 596–597, 2008.
- [19] J. J. Scragg, P. J. Dale, and L. M. Peter, "Synthesis and characterization of $\text{Cu}_2\text{ZnSnS}_4$ absorber layers by an electrodeposition-annealing route," *Thin Solid Films*, vol. 517, no. 7, pp. 2481–2484, 2009.
- [20] A. Ennaoui, M. Lux-Steiner, A. Weber et al., "Cu₂ZnSnS₄ thin film solar cells from electroplated precursors: novel low-cost perspective," *Thin Solid Films*, vol. 517, no. 7, pp. 2511–2514, 2009.
- [21] J. Madarász, P. Bombicz, M. Okuya, and S. Kaneko, "Thermal decomposition of thiourea complexes of Cu(I), Zn(II), and Sn(II) chlorides as precursors for the spray pyrolysis deposition of sulfide thin films," *Solid State Ionics*, vol. 141–142, pp. 439–446, 2001.
- [22] N. Kamoun, H. Bouzouita, and B. Rezig, "Fabrication and characterization of $\text{Cu}_2\text{ZnSnS}_4$ thin films deposited by spray pyrolysis technique," *Thin Solid Films*, vol. 515, no. 15, pp. 5949–5952, 2007.
- [23] Y. B. Kishore Kumar, G. Suresh Babu, P. Uday Bhaskar, and V. Sundara Raja, "Preparation and characterization of spray-deposited $\text{Cu}_2\text{ZnSnS}_4$ thin films," *Solar Energy Materials and Solar Cells*, vol. 93, no. 8, pp. 1230–1237, 2009.
- [24] Y. B. K. Kumar, G. S. Babu, P. U. Bhaskar, and V. S. Raja, "Effect of starting-solution pH on the growth of $\text{Cu}_2\text{ZnSnS}_4$ thin films deposited by spray pyrolysis," *Physica Status Solidi A*, vol. 206, no. 7, pp. 1525–1530, 2009.
- [25] N. Nakayama and K. Ito, "Sprayed films of stannite $\text{Cu}_2\text{ZnSnS}_4$," *Applied Surface Science*, vol. 92, pp. 171–175, 1996.
- [26] Q. Guo, H. W. Hillhouse, and R. Agrawal, "Synthesis of $\text{Cu}_2\text{ZnSnS}_4$ nanocrystal ink and its use for solar cells," *Journal of the American Chemical Society*, vol. 131, no. 33, pp. 11672–11673, 2009.
- [27] S. C. Riha, B. A. Parkinson, and A. L. Prieto, "Solution-based synthesis and characterization of $\text{Cu}_2\text{ZnSnS}_4$ nanocrystals," *Journal of the American Chemical Society*, vol. 131, no. 34, pp. 12054–12055, 2009.

- [28] C. Steinhagen, M. G. Panthani, V. Akhavan, B. Goodfellow, B. Koo, and B. A. Korgel, "Synthesis of $\text{Cu}_2\text{ZnSnS}_4$ nanocrystals for use in low-cost photovoltaics," *Journal of the American Chemical Society*, vol. 131, no. 35, pp. 12554–12555, 2009.
- [29] P. A. Fernandes, P. M. P. Salomé, and A. F. da Cunha, "Growth and Raman scattering characterization of $\text{Cu}_2\text{ZnSnS}_4$ thin films," *Thin Solid Films*, vol. 517, no. 7, pp. 2519–2523, 2009.
- [30] A.-J. Cheng, M. Manno, A. Khare, C. Leighton, S. A. Campbell, and E. S. Aydil, "Imaging and phase identification of $\text{Cu}_2\text{ZnSnS}_4$ thin films using confocal Raman spectroscopy," *Journal of Vacuum Science and Technology A*, vol. 29, no. 5, Article ID 051203, 2011.
- [31] A. C. Rastogi and S. Salkalachen, "Optical absorption behaviour of evaporated Cu_xS thin films," *Thin Solid Films*, vol. 97, no. 2, pp. 191–199, 1982.

